Charge ordering of magnetic monopoles in triangular spin ice patterns

A. Schumann[1], B. Sothmann[2], P. Szary[1], and H. Zabel[1]

[2]*Institut für Experimentalphysik/Festkörperphysik,*

Ruhr-Universität Bochum, 44780 Bochum, Germany

[2]*Theoretische Physik, Universität Duisburg-Essen and CeNIDE, 47048 Duisburg, Germany*

Abstract

Artificial spin ice offers the possibility to investigate a variety of dipolar orderings, spin frustrations and ground states. However, the most fascinating aspect is the realization that magnetic charge order can be established without spin order. We have investigated magnetic dipoles arranged on a honeycomb lattice as a function of applied field, using magnetic force microscopy. For the easy direction with the field parallel to one of the three dipole sublattices we observe at coercivity a maximum of spin frustration and simultaneously a maximum of charge order of magnetic monopoles with alternating charges $\pm$ 3.

In natural spin ice, magnetic ions form a network of corner-sharing tetrahedra such as holmium ions in holmium titanate[1]. Pairs of their magnetic moments point either in or out of the tetrahedra, which is then termed the "two in - two out" rule, following water ice, where on the average two hydrogen atoms point towards an oxygen ion and two point away. The two in - two out configuration is favored by the magnetic dipole-dipole interaction. Other configurations also occur frequently, such as three in and one out, or four in and none out. All these configurations carry a certain amount of frustration, but the best compromise still is the two in - two out rule, resulting in long range order. Modern lithographic techniques enable the fabrication of magnetic dipoles arranged on lattices with different symmetries, mimicking two dimensional projections of spin ice. Artificial square and triangular spin ice patterns are of particular interest in current research[2–5], because they provide a laboratory for the analysis of order and excitations in frustrated planar lattices with dipolar interaction[6].

Here we consider dipolar arrays placed on a honeycomb lattice, where each vertex consists of three equivalent dipoles enclosing an angle of 120°. The honeycomb lattice exhibits a fascinating variety and complexity of configurations and at the same time is highly frustrated. For each vertex there are a total of $2^3=8$ possible configurations. In analogy to the square spin ice, the spin ice rule for the honeycomb lattice is fulfilled if two dipoles point in and one points out, or vice versa. There are six configurations, which fulfill this rule (type II). The remaining two spin configurations (type I) with all three dipoles pointing either in or out, violate the spin ice rule. At the same time, the type I and II configurations define a certain value of "magnetic charges" (see Fig. 1). Assigning a charge +1 for dipoles pointing in and -1 for dipoles pointing out, type I vertices carry a charge of $\pm$ 3, and type II configurations a charge of $\pm$ 1. Vertices with charge $\pm$ 3 have no effective magnetic dipole and can be described as magnetic monopoles. It was recently pointed out that irrespective of the configurations adapted by an artificial spin ice pattern, the total charge of a pattern must be zero[6]. There is a another important prediction concerning spin ice configurations: charge order may occur independent of spin order[7]. In fact, in many systems charge order is found on different temperature scales than spin order. Examples are layered nickelates[8] or cobaltates[9]. In artificial spin ice patterns we cannot probe the temperature dependence of the ordering as thermal fluctuations are essentially suppressed by the large shape anisotropy. Instead we present field dependent studies, where spin order is induced in saturation and apparently maximum disorder is found at coercivity. However, charge order of magnetic

monopoles may still be present.

The honeycomb lattice has been studied theoretically by several authors[6,7,10] and was realized experimentally by lithographic means and investigated via magnetic force microscopy[3], Lorentz microscopy[4] and photoemission electron microscopy[11]. In the first two cases the dipoles were connected to each other, yielding the strong interaction limit, while in the third case only single up to triple honeycomb rings were investigated, excluding a statistical analysis. Here we present experimental realizations of magnetic dipoles arranged on a honeycomb lattice and we discuss the remanent state as well as the magnetization reversal in an external field. The reversal strongly depends on the field direction with respect to the main symmetry axes of the pattern, which are either [10] or [11]. In the [10] direction (hard axis), one dipole set of the three sublattices is perpendicular to the field direction and the other two are inclined at an angle of 30°. For the [11] direction (easy axis), one dipole set is parallel to the field direction, whereas the other two are inclined at an angle of 60°. We mainly focus on the [11] orientation and find that at coercivity the magnetization reversal passes through a highly charge ordered state.
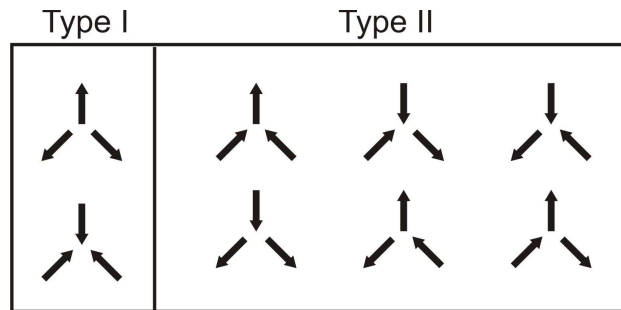

FIG. 1: Possible configurations of magnetic dipoles on a honeycomb lattice.

We deposited a 20 nm thick polycrystalline Fe film on a silicon substrate with a 5 nm thick Ta seed layer capped by a 2 nm thick Al_2O_3 layer for oxidation protection. The honeycomb patterns were prepared by means of e-beam lithography and ion beam etching, following procedures described elsewhere[12]. The final patterns consist of Fe-bars with dimensions length, width, and thickness of 3 μm, 0.3 μm and 20 nm, respectively. Here we discuss three honeycomb patterns with inter-island distances of 0.4 μm, 0.8 μm and 1.7 μm, SEM images of the patterns are shown in Fig. 2. The dipole configurations were imaged by a magnetic force microscope (MFM) at room temperature equipped with tunable in-plane magnetic field up to 1000 Oe and a rotation stage for aligning the pattern with respect to the external
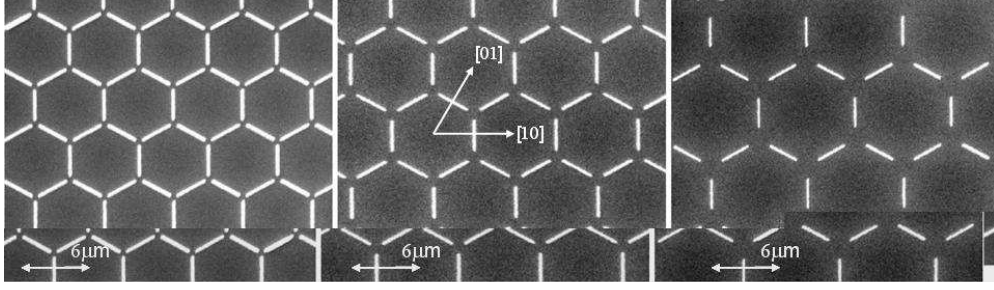
FIG. 2: SEM-image of three honeycomb lattices with different inter island spacing. Left: 0.4 μm, Middle: 0.8 μ m, Right: 1.7 μ m. Red bars indicate the scale and red arrows show the basis vectors of the honeycomb lattice.

field. In the MFM images each ferromagnetic island has at the ends a bright and a dark spot due to the emanating stray fields. This contrast confirms that for the aspect ratio chosen the islands are dominantly in a single domain state.

First we demagnetized the samples by driving the pattern through minor loops, meaning that we carefully decreased the applied magnetic field from well above saturation (1000 Oe) in small steps of 10 Oe while changing the direction of the magnetic field with each step[13,14]. Then we recorded MFM-images and analyzed the magnetic charge and the total magnetization of the scanned area by image processing. For evaluating the magnetization we assigned dipoles aligned parallel to the applied magnetic field with the normalized moment of $\pm$ 1, all others contribute a normalized moment of $\cos(\pm 60°, \pm 120°) = \pm 1/2$. By adding up all moments we derive a magnetization for each field value and thus a digital magnetic hysteresis curve.

For the [11] orientation (one sublattice aligned parallel to the applied magnetic field) and for large inter island distances we observe a nearly uncorrelated demagnetized state with a frequency of type I and type II vertices as expected for a random distribution. At the same time the demagnetized state fulfills the condition of charge neutrality. A representative example for the demagnetized pattern with a dipole separation of 0.8 μm is shown in Fig. 3(a).

We found that in the demagnetized state the charge and the magnetization is close to zero, which means that our demagnetization protocol was successful. Small deviations can be attributed to counting errors in the analysis software and/or local defects in the dipolar array. Upon increasing the external field parallel to the [11] direction, the magnetization
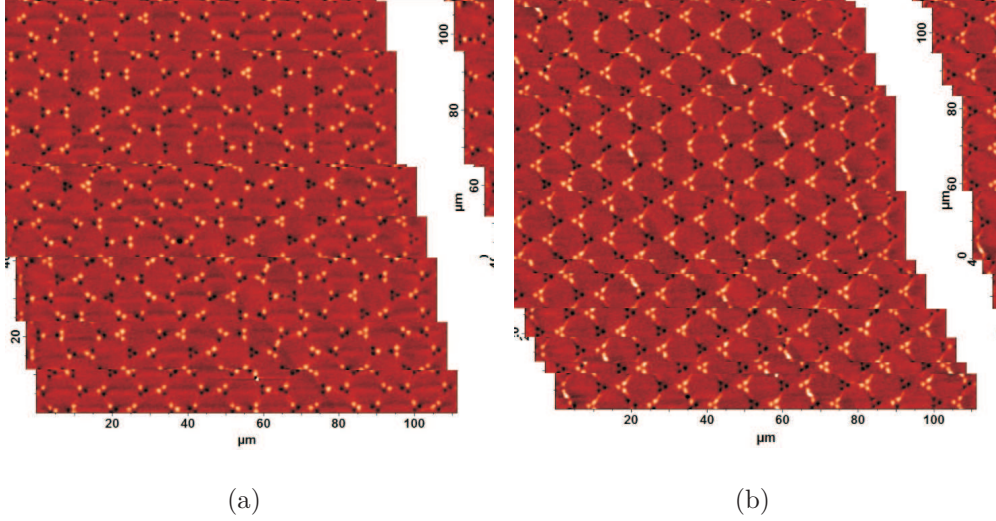
4

FIG. 3: (a): MFM-image of a demagnetized honeycomb lattice with inter-island spacing of 0.8 μm. (b): MFM-image of the honeycomb pattern with an inter-island distance of 0.8 μm taken at H_{ext} = -500 Oe. Note the high order of alternating ± 3 magnetic charges at the vertices.

first increases, drops again and finally reaches the saturation value. Fig. 4(a) reproduces the initial magnetization after the demagnetization procedure has been applied and a full loop for the honeycomb pattern with a dipole separation of 0.8 μm. Each point in this hysteresis is the result of a numerical evaluation of all dipoles in the scanned region of the pattern, as described before. Figure 4(b) shows the frequency of the type I state for this pattern and for the [11] field orientation. We notice that for the [11] orientation the frequency of type I vertices dramatically increases at coercivity in the descending as well as in the ascending branch of the hysteresis. The frequency of type I reaches values as high as 70%. This is rather surprising as type I vertices with a charge ± 3 violate the spin ice rule and present local maxima in the potential landscape for the magnetization reversal. At the same time we observe at coercivity a very high degree of charge order of magnetic monopoles with alternating charge ± 3. Figure 3(b) shows the 0.8 μm pattern at the field H_{ext} = -500 Oe descending from saturation. We infer from this image that coercivity in the honeycomb lattice is characterized not only by zero magnetization but also by the highest possible spin frustration with nearly complete charge order of magnetic monopoles.

The magnetization reversal through the charge ordered state can be understood by considering the coercivity fields of all three sublattices. The horizontal dipoles parallel to the external field direction switch first in a reversal field, followed by switching of the 60° in-

clined dipoles. As switching proceeds via a domain wall process, the effective switching field acting on the inclined dipoles is only half the value compared to that acting on the horizontal dipoles. Therefore between the first and second coercive field charge order may occur. We may speculate that in this region the frequency of type I states could increase to 100% and the charge order could be complete, if a certain distribution of switching fields and local defects in the pattern could be avoided. In this scenario maximum spin frustration coexists with complete charge order of magnetic monopoles.

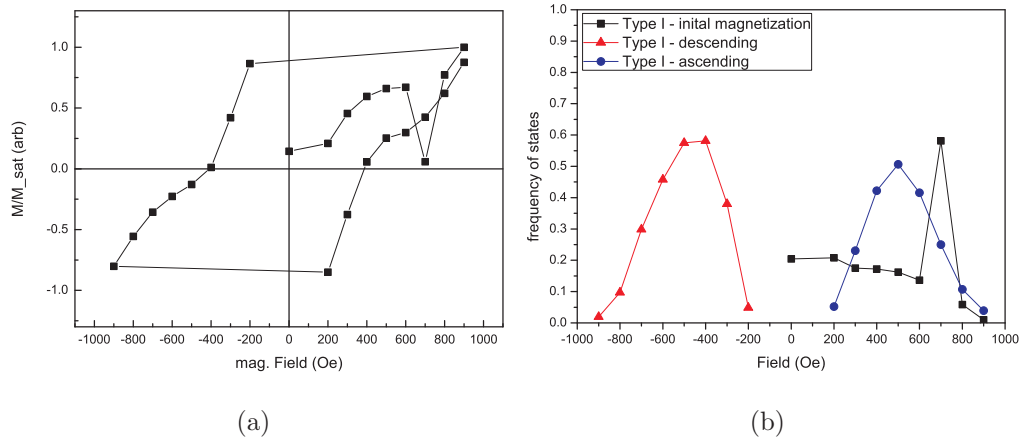(a)   (b)

FIG. 4: (a): Digital hysteresis loop for the magnetic field applied parallel to the [11] direction. (b): Frequency of the type I-state as a function of external field.

The magnetization reversal with the field applied parallel to the [10] direction follows a completely different path. The dipoles oriented perpendicular to the field direction do not switch at all in the field range applied here. They remain in a random orientation as established after the demagnetization procedure. The other dipoles inclined at an angle of $30°$ against the field direction switch more or less simultaneously. Thus neither magnetic order nor charge order can be established in this orientation. However, even if the perpendicular dipoles were first aligned parallel, charge order, as observed in the [11] direction at coercivity, would never prevail.

In summary, we have fabricated an artificial spin ice structure by arranging magnetic dipoles on a honeycomb lattice using e-beam lithography. We have studied the magnetization reversal of the honeycomb pattern for field directions parallel to the main symmetry directions of the triangular lattice, [10] and [11]. For the magnetic field applied parallel to the [11] direction we find at coercivity a highly ordered state of magnetic monopoles with

alternating charges ± 3. Perfect order is only hindered by local defects and by a distribution of switching fields. In contrast, for fields applied along the [10] direction, a charge ordered state can not be established.

———————————————

[1] A.P. Ramirez, A. Hayashi, R.J. Cava, R. Siddharthan, and B.S. Shastry, Nature **399**, 333 (1999).

[2] R.F. Wang, C. Nisoli, R. S. Freitas, J. Li, W. McConville, B. J. Cooley, M. S. Lund, N. Samarth, C. Leighton, V. H. Crespi, and P. Schiffer, Nature **439**, 303 (2006).

[3] M. Tanaka, E. Saitoh, H. Miyajima, T. Yamaoka, and Y. Iye, Phys. Rev. B **73**, 052411 (2006).

[4] Y. Qi, T. Brintlinger, and J. Cumings, Phys. Rev. B **77**, 094418 (2008).

[5] H. Zabel, A. Schumann, A. Westphalen, and A. Remhof, Acta Physica Polonica A **97** 2000 (2008).

[6] G. Möller and R. Moessner, Phys. Rev. Lett. **96**, 237202 (2006).

[7] G. Möller and R. Moessner, Phys. Rev. B **80**, 140409 (R) 2009).

[8] Gianluca Giovannetti, Sanjeev Kumar, Daniel Khomskii, Silvia Picozzi, and Jeroen van den Brink, Phys. Rev. Lett. **103**, 156401 (2009).

[9] G. Lang, J. Bobroff, H. Alloul, G. Collin, and N. Blanchard, Phys. Rev. B **78**, 155116 (2008).

[10] A.S. Wills, R. Ballou, and C. Lacroixet, Phys. Rev. B **66**, 144407 (2002).

[11] E. Mengotti L. J. Heyderman, A. Fraile Rodriguez, A. Bisig, L. Le Guyader, F. Nolting, and H. B. Braun, Phys. Rev. B **78**, 144402 (2008).

[12] A. Remhof, A. Schumann, A. Westphalen, H. Zabel, N. Mikuszeit, E. Y. Vedmedenko, T. Last, and U. Kunze, Phys. Rev. B **77**, 134409 (2008).

[13] X. Ke, J. Li, C. Nisoli, Paul E. Lammert, W. McConville, R. F. Wang, V. H. Crespi, and P. Schiffer, Phys. Rev. Lett. **101**, 037205 (2008).

[14] R. F. Wang, J. Li, W. McConville, C. Nisoli, X. Ke, J. W. Freeland, V. Rose, M. Grimsditch, P. Lammert, V. H. Crespi, and P. Schiffer, J. Appl. Phys. **101**, 09J104 (2007).